A THEORETICAL APPROACH TO SYNTHETIC VASCULAR GRAFT DESIGN: SURFACE MICRO-TOPOGRAPHY OPTIMIZATION FOR PROMOTING THE RETENTION OF ENDOTHELIAL CELLS

By

Christina C. Marasco

Thesis

Submitted to the Faculty of the

Graduate School of Vanderbilt University

in partial fulfillment of the requirements

for the degree of

MASTER OF SCIENCE

in

Biomedical Engineering

May, 2007

Nashville, Tennessee

Approved:

Professor V. Prasad Shastri

Professor Robert J. Roselli

ACKNOWLEDGEMENTS

My gratitude is offered to the Vanderbilt University Department of Biomedical Engineering for providing me with Teaching Assistantships that have allowed me to expand my knowledge and teaching skills in ways I never thought possible. Additionally, I appreciate the support of the Vanderbilt Institute for Integrative Biosystems Research and Education grant that has allowed me to move forward with my research.

The aid of my advisor, Dr. Shastri, has been indescribable. The guidance from Dr. Roselli in writing this thesis, as well as in my graduate career as a whole, has been extremely valuable. I am greatly indebted to Dr. Ashley Weiner, without whom I would be in the dark. I would also like to thank Aditya Kalavagunta for his priceless assistance in navigating COMSOL Multiphysics and Dr. Jason Nichol for taking the time to answer my questions.

Where of course would any of us be without the love and support of our family and friends. This leads me to thank my husband, Derek, my parents and siblings, and all of my friends whose presence in my life is genuinely treasured. (And because I regard your friendships so highly, I will never ask you to read this thesis.)

Finally, but most importantly, I must thank God for giving me talents and abilities, as well as the ambition, to reach this point in my career. For it is truly all for your glory that I continue to pursue this field of study.

TABLE OF CONTENTS

LIST OF FIGURES

CHAPTER I

INTRODUCTION

Cardiovascular Disease

Cardiovascular diseases, including coronary artery disease and peripheral vascular disease, are the leading cause of death in the Western world, accounting for almost 30% of all deaths [1]. An estimated 1 in 5 US residents suffer from some form of cardiovascular disease, bringing the total cost of treatment to around $300 billion each year [2]. Such disease states are a result of the gradual deposition of plaque, a hard cholesterol substance, leading to alterations in the physiological flow of blood through vessels. These depositions along the vessel walls result in the narrowing of the vessel, referred to as stenosis. Due to increased shear rates in the partially occluded regions, the promotion of platelet accumulation is seen, leading to thrombus formation in the vessel.

Treatment strategies include types of preventative medications, including those that inhibit the formation of various factors involved in clotting; those that inhibit platelet-platelet interactions, Plavix, for example; those that interfere with the binding ability of clotting factors to platelets; and also those that cause a reduction in blood viscosity, such as heparin. These medications, however, do not typically break down or prevent the deposition of plaque. Statins, a class of drug capable of reducing cholesterol levels in the blood, have been shown to stabilize plaque, prevent thrombosis, and improve the overall function of the endothelium [3].

For a severe stenosis, more vigorous treatment strategies are employed including angioplasty, endovascular stenting, and bypass surgery. The latter option tends to be the most frequented [4, 5], with over 400,000 coronary artery bypass surgeries performed annually in the United States [6]. Blumenthal *et al*. report that patients who underwent coronary artery bypass surgery had a greater event-free survival rate than those who underwent either coronary angioplasty or medical treatment with statins [5]. Achieving long-term success with angioplasty is limited based on the high occurrence of restenosis [2, 7]. While the use of stents to prevent reocclusion has improved success rates, in-stent restenosis has also emerged as a limitation of this treatment option [7]. Extensive research and clinical trials have been conducted and will continue to be performed in order to investigate both new strategies and improvements of the current options for the treatment of cardiovascular diseases.

Clotting and Thrombosis

Regions of damaged endothelium and plaque deposition are highly susceptible to thrombus formation. This process begins with the adhesion of platelets to the dysfunctional wall of the vessel, causing them to become activated and release ADP which in turn triggers nearby platelets to become sticky and aggregate [8, 9]. This process of thrombus formation rapidly proceeds and is unpredictable due to altered platelet reactivity [9]. In normal hemostasis, a similar process occurs, however, a properly functioning endothelium will release prostacyclin in order to inhibit platelet aggregation, thus the size of the plug formation is limited [8]. The coagulation cascade, in which blood becomes a solid, follows the plug formation in order to stabilize the clot. In the presence

of elevated shear stress or infection, the thrombus or clot may become dislodged and then travel downstream to smaller vessels where it may completely block blood flow, causing an infarction [8].

Vascular Grafts

Autologous vascular grafts

Autografts, namely the free radial and internal mammary arteries and the saphenous vein, are typically used in coronary artery bypass surgeries [6, 10]. It has been reported that reocclusion occurs in about 50% of vein grafts within 10 years of the initial surgery, while the early and late patency rates of internal mammary artery grafts are greater than 90% [11]. However, in some patients these vessels are not available for use as a result of advanced diseased states or previous bypass surgery [12, 13]. Thus, an alternative small-diameter graft is needed, specifically synthetic or tissue-engineered vascular graft.

Alternative vascular grafts

While large-diameter (>6 mm) engineered vascular grafts, typically made of Dacron or expanded polytetrafluoroethylene (ePTFE), have had some success, small-diameter versions are plagued with thrombogenicity and neointimal hyperplasia, among other modes of failure [10, 13-15]. Although the most important characteristics of the optimal small diameter vascular graft are debatable, researchers tend to agree that this substitute should posses the following criteria: nonthrombogenic luminal surface,

biocompatible, and compliant [10, 12, 13, 16, 17]. There have been many different tissue engineered approaches to the production of a viable small diameter vascular graft alternative, the majority of which use endothelial cells as the blood-contacting surface. Such tactics include, but are not limited to, the use of decellularized, tubular tissues as scaffolds, the use of biodegradable polymer scaffolds, the use of permanent synthetic scaffolds, and additionally, non-scaffold based approaches.

Decellularized tissues. The use of decellularized tissues for the graft construct is advantageous since they are constituted purely by extracellular matrix. The tissue source may be autologous or xenogeneic vascular tissue or even small intestinal submucosa [12]. The decellularized version of these tissues is implanted with the notion that endothelial cell migration in the host will recellularize the tissue [12]. Unfortunately, decellularized xenograft implantation tends to lead to aneurysm and thrombus formation, however patency rates in a sheep model are increased when endothelial cells are pre-seeded [18]. Additionally, the use of pre-seeded allogenic grafts instead of xenografts result in short-term patency rates in a porcine model that are approaching those for saphenous vein grafts, yet still less than those for arterial grafts [19]. While this approach to the creation of small diameter vessel substitutes is promising, long-term studies are necessary in order to demonstrate the true potential of this method.

Biodegradable polymer scaffolds. Biodegradable polymer scaffolds are used as supports on which to seed cells, usually both smooth muscle cells and endothelial cells, and as the new vessel is formed, the polymer degrades [12, 20]. Numerous polymers and co-polymers have been studied for use in this application including polyglycolic acid [12, 17, 21]. One possible issue with this type of method is in the degradation of the polymer

scaffold itself. While it is advantageous that polymer properties are easily tunable, incomplete degradation may lead to an immune response [20]. Multiple studies have shown outstanding patency rates [22-25], yet assessing long-term function of this vessel substitute, particularly in a patient, is difficult, but a necessity for comparison to autologous grafts.

Permanent synthetic scaffolds. The use of permanent synthetic scaffolds on which to seed vascular cells is another method for the creation of small-diameter grafts. This approach is based on the work of Weinberg and Bell [26] in which the lumen of a tubular collagen scaffold, contracted by smooth muscle cells and reinforced by a Dacron mesh, was seeded with endothelial cells. Once implanted, inhibited remodeling of the graft vasculature due to the presence of the permanent scaffold, Dacron, may be of concern in the opinion of some researchers [20], however, it is the opinion of others that the biostability provided by the polymeric scaffold is of greater importance as the degradation of the polymer scaffold will lead to a dramatic alteration of the graft properties [17]. Although large diameter synthetic grafts have historically been made from Dacron or ePTFE, small diameter variations turn to elastomeric polymers, such as polyurethane, for their compliancy and biocompatibility. Modifications of polyurethane seek to improve the nonthrombogenicity and stability of the scaffold. For instance, carbonate-based polyurethanes have been demonstrated to be patent in a canine model for more than 36 months and are now in clinical trials [17, 27]. Additionally, new methods of creating specific polymer structures are being developed to aid in mimicking the structure of a native vessel. Electrospinning and self-assembly are examples of methods by which the creation of fibers with diameters similar to those of the extracellular matrix is

achieved [12]. These fibers are typically made of polyester, collagen, and fibrinogen [12]. Researchers have not failed to extensively explore the use of permanent synthetic scaffolds, however this area of ongoing research is expansive, leaving much to be discovered.

Non-scaffold based approach. An additional method for small-diameter vascular grafts is that which lacks the use of a scaffold entirely, a completely biological graft. Instead, a mold or mandrel is used to provide a framework for a developing graft and then removed prior to implantation. L'Heureux *et al*. developed a method of layering sheets of smooth muscle cells and fibroblasts around a cylindrical mandrel [28]. Once the mandrel was removed, endothelial cells were seeded on the luminal surface. One limitation of this particular method is the lengthy culture time required for each layer added to the construct, while the benefits of using a completely autologous graft are clearly in the lack of immune response to the implant.

Although an enormous amount of research has been conducted with the goal of creating a viable small-diameter graft alternative and many different types of constructs have been developed, a functional alternative capable of eliciting similar success rates to autologous grafts remains to be found. The current methods of testing the potential alternative vascular grafts, as well as assessing their long-term patency, in this author's opinion, are not adequate, and thus, hinder the progression of the field. Additionally, the criteria for an ideal alternative graft listed above is a shortened version, excluding those criteria debated by experts, for example, the ability to exhibit physiological properties such as vasoconstriction [12] and possessing a burst strength similar to that of the native vessel [15]. The determination of a set of criteria, experimentally shown to be necessary

characteristics of an ideal graft, will allow for a more focused effort in the development of an alternative vascular graft.

Reducing Thrombogenicity of Vascular Grafts

Surface modification

The primary mode of failure of engineered vascular grafts is occlusion due to thrombogenicity. A technique for rectifying this situation is to coat the synthetic or natural polymer scaffold with anticoagulants or anti-platelet agents, or to disperse these within the material [29]. Keuren *et al.* performed a study in which collagen was heparinized [30]. They observed no change in platelet adhesion; however, the absence of thrombin generation led them to conclude that heparinizing collagen improves thromboresistance. In another study, dipyridamole, an inhibitor of platelet aggregation and activation, was attached to a polyurethane surface, which resulted in decreased thrombogenicity when exposed to platelet-rich plasma [31]. Yoneyama *et al.* have investigated the use of a nonthrombogenic phospholipid polymer, 2-methacryloyloxyethyl phosphorylcholine (MPC), in a copolymer form with polyurethane [32]. The structure of the MPC polymer resembles that of the cell membrane and is capable of inhibiting platelet activation and aggregation, making it a useful material for vascular graft prostheses. These methods of modifying blood-contacting surfaces have not shown to be adequate for reducing thrombogenicity. Instead they are usually incorporated with other methods of reducing thrombogenicity, for instance, endothelial cell seeding.

Endothelial cell seeding

Because endothelial cells are the blood-contacting surface of a native vessel, the motivation to seed synthetic and tissue engineered vessels with these naturally nonthrombogenic cells is clear. This technique was initiated almost 30 years ago by Herring *et al.* [33]. As the introduction of foreign cells into a patient elicits an immune response, it is ideal to harvest the patient's own cells for seeding of the graft lumen prior to implantation. Typically, autologous endothelial cells are harvested from vessels, such as the saphenous vein, or omental adipose tissue [34, 35]. When a limited supply of endothelial cells is available in a given patient, it is possible to use cell culture techniques in order to expand the population. Although doubling time is reported to be 24 hours, the need to perform any number of passages disqualifies grafts requiring a culture period from use in an emergency situation [14, 15, 35]. In these types of procedures, a single-stage seeding process must be performed in which the cells must be harvested, seeded onto the graft, and the implantation of the graft must all be done within the length of the surgery [14, 36]. A two-stage seeding method, on the other hand, is classified as one involving tissue culture time [14, 36] and has been shown to improve clinical outcomes in small diameter vascular grafts [37]. The actual technique of cell seeding can be accomplished by a number of methods. The gravitational method involves filling the graft lumen with a suspension of endothelial cells, often in tissue culture media or blood, and rotating the vessel for a specified length of time [35]. Hydrostatic seeding methods employ the use of a pressure gradient applied across a porous graft material in order to compel endothelial cells suspended in medium to move onto the luminal surface of the vessel [35]. The length of time over which incubation should be performed once the cells

have been seeded is debated and also related to the retention of cells [35, 36]. Electrostatic seeding is another highly useful technique in which an electric field is applied to the scaffold in order to induce a more positive surface charge that enhances endothelial cell attraction to the surface [35]. When endothelial cells on a polymeric substrate are subjected to the flow conditions typical in small-diameter vessel, poor endothelial cell retention is seen, especially when the seeding density is low [12, 17]. This allows for contact between blood and the bare substrate, resulting in platelet adhesion that eventually leads to thrombosis. Thus, methods of improving endothelial cell retention must be developed.

Improving Endothelial Cell Retention

Chemical surface modification

One possible method of improving endothelial cell adhesion to surfaces, and thus a means of preventing thrombotic occlusion in vascular grafts, is to alter the surface through the deposition of proteins or peptide sequences. Commonly, proteins such as fibronectin, gelatin, collagen, laminin and fibrin are used to coat the surface of the substrate prior to seeding with cells [14, 17, 35]. Fibronectin coatings have shown to be the most successful for improving endothelial cell retention. Increased cell attachment is typically seen when fibronectin is used in combination with another protein or ligand [38]. Extensive investigation into the use of the RGD peptide sequence, the functional ligand of fibronectin, to aid in cell adhesion has been accomplished [39-43]. Other peptide sequences found to enhance endothelial cell adhesion include REDV [44],

another fibronectin ligand, and YIGSR [45], derived from laminin. While extensive investigation into these coatings has been conducted, success has been limited as high flow rates cause their detachment [14, 17] and in some cases, poor specificity between the ligand or protein and the cell allows for undesirable platelet adhesion [34].

Flow conditioning

Another method used to enhance endothelial cell attachment to a polymer scaffold is the process of flow conditioning by which cells are exposed *in vitro* to flow-induced shear stress post-seeding procedure. Ott *et al.* exposed cells seeded on polyurethane vascular grafts first to a shear stress of 1-2 dyn/cm^2 for 3 days, then to a stress of 25 dyn/cm^2 for an additional 3 days, and showed that this enabled enhanced retention [46]. Isenberg *et al.* developed a system to expose endothelial cells to various physiological shear stress conditions, including both steady and pulsatile flow at various flow rates, resulting in the development of an endothelial cell monolayer with adhesion strengths adequate to withstand physiological shear stresses [47]. Dardik *et al.* showed that a shear stress of 25 dyn/cm^2 applied to cells over a period of 3 days resulted in the maintenance of a confluent cell monolayer for 3 months after implantation [48]. Pulsatile, low shear stresses of 1-2 dyn/cm^2 applied for 7 days were shown by Baguneid *et al.* to enhance endothelial retention in vitro when subjected to mean shear stress of around 9 dyn/cm^2 [49]. Additionally, it has been shown that shear stress influences the phenotype of endothelial cells, including the ability to adhere to a surface, and may be used to control vascular cell differentiation [50].

Physical surface modification

Physical methods of altering the vascular graft substrate have also been attempted through modification of surface topography. In work by Uttayarat *et al.* [51], micro- and nano-grooves in poly(dimethylsiloxane) (PDMS) were used to align endothelial cells, and they further observed that patterning did not have an adverse effect on cell densities as comparable values were seen both after 48 and 72 hrs in patterned and unpatterned substrates. Additionally, they reported that focal adhesions were seen in the bottoms of 1-μm deep channels, but surprisingly not in those of the 5-μm deep channels, causing them to speculate that the decrease in channel width with increasing depth may have prevented these adhesions from forming. Gray *et al.* showed that endothelial cells preferentially accumulate on stiffer regions of a PDMS substrate suggesting that material stiffness may be used to promote preferential endothelial cell adhesion [52]. Goodman *et al.* created a polyurethane scaffold micro-patterned to mimic the natural sub-endothelial extracellular matrix topography [53]. Endothelial cells seeded on these surfaces were found to more closely resemble those attached to the native extracellular matrix, suggesting that mechanical cues from textured surfaces can alter cellular phenotype. Fujisawa et al. created a surface texture consisting of regularly spaced tapered micro-fibers capable of controlling the thickness of psuedo-neointima, resulting in an increase in the cellular migration onto the textured surface [54]. Bettinger *et al.* developed a rounded surface topography that was able to promote the alignment and elongation of endothelial cells speculated to be a result of the ability of filopodia to sense changes in surface topography [55]. Finally, Daxini *et al.* created a pattern of microchannels with a defined geometry in order to create regions of lowered shear stress to prevent delamination of endothelial cells

[56]. While the idea of contact guidance has long since been used to explain cellular behavior, limited work has been performed specifically on endothelial cells. It is a field in need of exploration, as enhanced attachment and alignment allow for the creation of a sustained, confluent, nonthrombogenic endothelium that is highly desirable in the created of a clinically relevant alternative vascular graft.

Endothelial Cell Response to Shear Stress

In their native environment, endothelial cells are subjected to various mechanical forces, including shear stress, the viscous dragging force created by the flow of blood. It has been shown by many that endothelial cells, when exposed to positive shear stress, will reorient to align their longitudinal axis parallel to the flow direction [57, 58]. Depending on the vessel size and location, the flow rate and wall shear stress can be markedly different. For example, flow through larger (>6 mm), relatively straight arteries is steady, laminar flow, which exerts mean positive shear stress on the endothelium [59]. However, flow through the bifurcation in the carotid arteries is unsteady and known to cause regions of flow separation and secondary flows, and is characterized by low mean wall shear stress [60]. Lower shear stress at the vessel wall, as well as flow separation and reversal, has been shown to coincide with atherosclerotic prone regions [58]. Typical arterial shear stress falls into the range of 10-70 dyn/cm^2 [58]. Physiological or elevated shear stress is thought to have an atheroprotective effect, as the expression of an atheroprotective gene is induced by shear stresses above 15 dyn/cm^2, while an atherogenic endothelial cell phenotype is promoted by shear stresses below 4 dyn/cm^2 [58, 59]. For instance, one crucial function of endothelial cells is the secretion of the

vasodilator nitric oxide, and an increase in nitric oxide secretion is seen with physiological and elevated levels of shear stress [59, 61]. Because nitric oxide inhibits platelet aggregation, its presence reduces the possibility of thrombosis [2]. Additionally, these same levels of shear stress have been shown to decrease endothelial cell turnover [58]. Many have reported that apoptosis in endothelial cells may be caused by a lack of sufficient shear stress [62, 63]. It is evident that aberrant shear stress levels, whether low or high, can result in undesirable behavior of endothelial cells. Since those endothelial cells are needed to maintain the non-thrombogenic surface of the vessel lumen, preserving physiological shear stress levels is paramount.

Fluid Dynamics of Plate Flow

In order to determine the level of shear stress contacting endothelial cells seeded on a vascular graft lumen, a computational model of the fluid flow through the vessel can be created. Blood flow in a vessel is often modeled as pressure-driven flow in a cylindrical tube, with blood typically modeled as an incompressible, Newtonian fluid. Many researchers employ in vitro studies to investigate the cellular response to flow and the corresponding shear stress with the use of parallel plate flow chambers [64-66]. Thus, mathematical models that describe flow behavior in these chambers of defined geometry may be of use to predict and correlate changes in endothelial cell function and shape as a response to the particular flow conditions, as well as the resulting shear stress. A common model employs the use of the Navier-Stokes equation for steady, pressure-driven flow between two parallel plates with a no slip boundary condition applied to the surface of the plates, resulting in parabolic Poiseuillian flow [67]. In such models of flat plate flow,

the calculation of the wall shear stress may be easily accomplished from a known velocity gradient normal to the surface. However, when various types of surface roughness, such as waves [68], are incorporated into the plate, the flow at the surface is altered and direction normal to the surface is not the same in all locations, increasing the complexity in the determination of wall shear stress. Usha *et al.* found, through the use of a mathematical model, that increasing the waviness of a surface causes a decrease in shear stress in the valley sections and an increase in shear stress at the crests [68]. In their model of flow over a rigid, circular cell adhering to a wall, Gaver *et al.* reported that as the size of the cell is increased, an elevation in wall shear stress on that cell occurs [67]. It has been demonstrated that alterations in the topography of a surface alters the velocity gradient near the surface resulting in changes in the wall shear stress.

Specific Aim

It has been shown in previous work in our laboratory that structural surface modification allows for enhanced endothelial cell retention. Polyurethane films with a V-shaped microchannel were found to, upon seeding with endothelial cells, exhibit 92% retention, compared to 58% retention on unpatterned surfaces [56]. However, regions of high wall shear stress (around 150 dyn/cm^2) were shown to be concentrated at channel edges [56]. Since alterations in surface topography can affect wall shear stress, channel geometry will be altered in such a way as to select for a range of physiological stresses. The specific aim of this work is to alter channel geometry, and thus, shear stress, for the purpose of designing a new vascular graft lumen surface topography that produces wall shear stress values in the physiological range.

CHAPTER II

OPTIMIZATION OF VASCULAR GRAFT LUMEN MICRO-TOPOGRAPHY FOR PROMOTING THE RETENTION OF ENDOTHELIAL CELLS: A THEORETICAL TREATMENT

Abstract

The failure of synthetic vascular grafts due to de-endothelialization of the lumen as a result of exposure to fluid-induced shear stress prevents the widespread use of such grafts as small-diameter vessel replacements. Physical surface modification, an approach that seeks to alter the topography of the luminal surface, has been investigated as a method of reducing de-endothelialization under physiological stresses. Based on prior experimental evidence supporting this approach, computation fluid dynamics was used to investigate the impact of selected channel geometry parameters (wall angle, channel width, depth, and radius of curvature) on fluid flow and the resulting wall shear stress. Optimization of these parameters was performed in order to determine if micro-topographical modification of the lumen wall could alter fluid flow in a manner such that favorable conditions for both endothelial cell retention and stimulation are produced. It was found that a 50% decrease in the wall angle, width, and depth causes a decrease in maximum wall shear stress of around 8%, 8%, and 15%, respectively. Additionally, increasing the radius of curvature at the top and bottom edges by 50% results in a 10% decrease in maximum wall shear stress. These results indicate that it may be possible to tune the lumen micro-topography in order to provide a desired range of stresses, and subsequently reduce thrombogenicity by enhancing endothelial cell retention and function.

Introduction

Coronary artery disease and peripheral vascular disease account for almost 30% of all deaths in Western society [1]. When physiological flow of blood through vessels is altered by the deposition of plaque, such diseases can result. Restoration of blood flow in occluded vessels can be accomplished through several treatment options including angioplasty, stenting, and bypass surgery. Annually, over 400,000 coronary artery bypass surgeries performed in the United States [6]. The free radial and internal mammary arteries and the saphenous vein are the autologous grafts of choice for use in bypass surgeries; however, there is limited availability of these grafts as a result of advanced diseased states or previous bypass surgery [6, 10]. Additionally, compliance mismatch of the graft with the vessel at the site of anastomosis can occur [69]. These issues have prompted the development of alternative grafts, specifically a synthetic or tissue-engineered alternative.

While large-diameter (>6 mm) engineered vascular grafts, typically made of Dacron or expanded polytetrafluoroethylene (ePTFE), have had good success, small-diameter versions are plagued with a high rate of failure due to thrombogenicity of the luminal surface, among other modes of failure [10]. Since one of the functional requirements for a vascular graft is to be able to provide a nonthrombogenic luminal surface, there have been many attempts to seed the surface with endothelial cells [14]. However, when subjected to the flow conditions typical of smaller diameter vessels, poor endothelial cell retention is seen from the already low seeding density, allowing blood to contact the bare substrate, resulting in platelet adhesion that eventually leads to thrombosis [12, 17].

One possible method of improving endothelial cell adhesion to surfaces, and thus a means of preventing thrombotic occlusion in vascular grafts, is chemical surface modification. Commonly proteins such as fibronectin and gelatin are used to coat the surface of the substrate prior to seeding with cell [17]. Extensive investigation into the use of the RGD peptide sequence, the functional ligand of fibronectin, has been accomplished. However, success with these types of coatings is limited as high flow rates cause their detachment [17].

As discussed earlier, physical methods of altering the vascular graft substrate have also been attempted. Substrates with specific surface porosities have been created to allow endothelial cells to be incorporated into the substrate itself. Unfortunately, the physical difference between these surfaces and a native vessel is an inherent problem with this design [17]. Uttayarat *et al.* have used grooves ranging from 5 μm to 200 nm in depth to show the ability of endothelial cells to align in channels based on the surface topography of the substrate [51]. Both focal adhesions and, accordingly, cell alignment were evident in the 1-μm deep channels. Past work in our laboratory has shown that physical surface modification effectively alters fluid flow near the vessel wall, producing regions of diminished shear stress, which leads to enhanced endothelial cell retention [56]. Limitations of the previous design include the presence of high wall shear stress (around 150 dyn/cm^2) concentrated at channel edges and stagnant flow in the channel bottoms. In the earlier study, the channel edges were observed to be the leading edge in de-endothelialization due to the elevated shear stress imposed upon the cells in these regions.

Furthermore, it has been established that normal endothelial cell function, such as secretion of NO, will be deficient in the absence of an adequate level of shear stress [59, 61], and many have reported that apoptosis in endothelial cells may be caused by a lack of sufficient shear stress [62, 63]. Typical arterial shear stress falls into the range of 10-70 dyn/cm^2 [4, 58].

In the present work, channel geometry is further investigated in order to lay the foundations for the design of a vascular graft lumen that will prevent endothelial cell loss and stimulate normal NO production. The following criteria is used to accomplish this: reduction of high shear stress regions at channel edges to 70 dyn/cm^2 or less, channel bottom must experience an average shear stress of at least 10 dyn/cm^2, and minimize plateau regions to allow endothelial cell sheets to have numerous anchor points in areas of lower shear stress. The goal of this work therefore, is to optimize the microchannel geometry in order to create a suitably stressed environment to both harbor endothelial cells and promote their normal function.

Methods

A computational model was used to describe the flow of blood over the physically modified graft surfaces. Blood was modeled as an incompressible, Newtonian fluid with a density of 0.925 g/ml and a viscosity of 1 x 10^{-3} Pa s. Three-dimensional models of the channel geometry shown below in Figure 1 were generated in Pro/Engineer. Determination of the flow field for a single channel was accomplished by using Comsol Multiphysics v3.2b to solve the 3-D steady state Navier-stokes equation for parallel flow.

$$\nabla p = \mu \nabla^2 \bar{v} + \rho \bar{g} \tag{1}$$

where ρ is the fluid density, μ is the viscosity of blood, $\bar{v}$ is the fluid velocity vector, ∇p is the pressure gradient, and $\bar{g}$ is the gravity vector, which will be neglected as the effects of gravity are assumed to be negligible with respect to the 1st and 2nd terms in Equation (1).

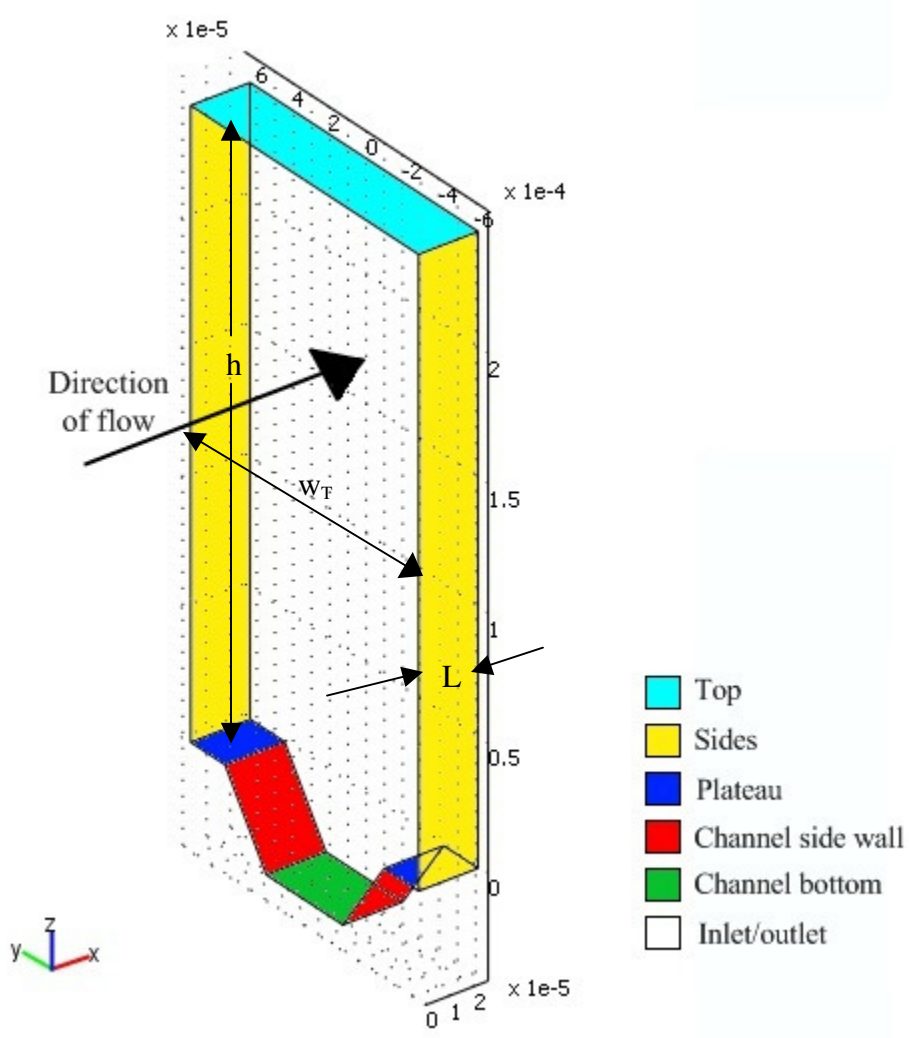

Figure 1. Representative channel model showing the nomenclature used to describe sections of the model. The overall width of the model is described by w_T, h is the height of the model from the plateau region (blue) to the top (turquoise), the latter being the location of maximum velocity in the channel, and L is the length of the model in the x-direction. The units of the model are given in meters.

The following boundary conditions were applied to the model to solve the steady state Navier-stokes equation.

1. The flow was assumed to be fully developed at the inlet and outlet of the channel model (shown in white).

$$v_y = v_z = 0 \tag{2}$$

2. The sides of the model (shown in yellow) were prescribed as symmetrical about the z-axis.

$$\left.\frac{\partial v_x}{\partial y}\right|_{y=\frac{w_T}{2}} = \frac{\partial v_x}{\partial z} y\Big|_{y=\frac{-w_T}{2}} = 0 \tag{3}$$

3. The top of the model (shown in turquoise), which would correspond to a plane in the centerline of parallel plate flow, was set as symmetrical about the y-axis.

$$\left.\frac{\partial v_x}{\partial z}\right|_{z=h} = 0 \tag{4}$$

4. The no slip boundary condition was set at the plateau (shown in blue), channel side walls (shown in red), and channel bottom (shown in green) regions.

$$v_x\big|_{wall} = 0 \tag{5}$$

5. A pressure gradient was applied in the x-direction corresponding to a velocity of 0.7 m/s in the x-direction at the top of the model (shown in turquoise).

$$\Delta p\big|_x = p\big|_{\mathrm{x=o}} - p\big|_{\mathrm{x=L}} \tag{6}$$

$$v_x\big|_{z=h} = 0.7\mathrm{m/s} \tag{7}$$

Each 3-D model investigated was sectioned into numerous discreet elements, a mesh, in order to solve for the flow field. For a single channel, the number of elements was on the order of 10^3, and for a geometry containing multiple channels the number of elements was an order of magnitude higher. Once the simulation was performed, the wall shear stress was determined by using the following equation:

$$\tau_{wall} = \mu \left. \frac{d\bar{v}}{dn} \right|_{n=0}, \tag{8}$$

where τ_{wall} is the wall shear stress in dyn/cm^2, μ is the viscosity of blood, and $\frac{d\bar{v}}{dn}$ is the velocity gradient with n being the direction normal to the channel plateau, side wall, or bottom.

The effects of channel geometry on shear stress and flow were investigated. The parameters as depicted in Figure 2 (depth, width, wall angle, and curvature) were varied, one at a time, in order to determine the effect on wall shear stress.

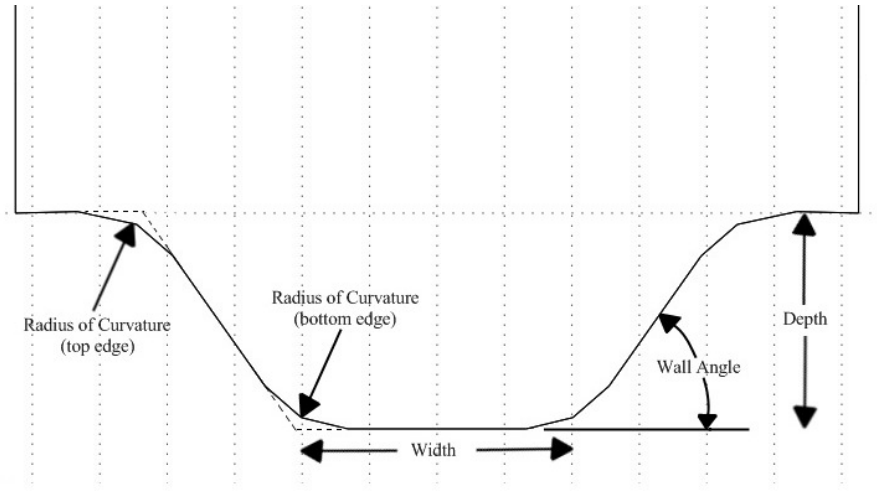

Figure 2. Depiction of the microchannel geometry features to be investigated. Wall angles studied ranged from 25º to 125.3º, channel widths rangde from 22 to 62 μm, channel depths ranged from 12 to 52 μm, and the radius of curvature at the top and bottom edges will range from 0 to 15 μm.

The wall angle of the channel is defined as the angle from the positive y-axis to the channel side wall. Microchannel models were created with wall angles ranging from 25º to 125.3º. Channels with a wall angle between 10º and 90º are referred to, herein, as V-shaped channels. Those with wall angles greater than 90º are referred to as inverted V-shaped, and a channel with a wall angle of 90º is referred to as square. See Figure 3 for examples.

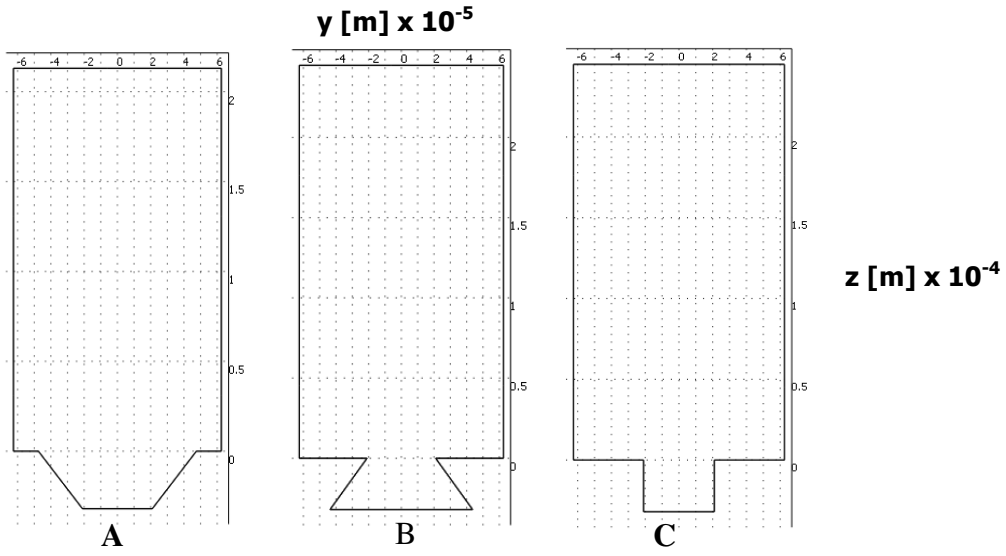

Figure 3. Examples of the three types of channel models that were investigated, V-shaped channel with wall angles less than 90º (**A**), inverted V-shaped channel with wall angles greater than 90º (**B**), and Square channel model with a wall angle of exactly 90º (**C**).

The next parameter investigated was the radius of curvature of the channel, which can be defined as the smoothness of the transition between the plateau region and the channel side wall, and between the channel side wall and channel bottom, respectively. The intersecting edge of the former is referred to as the top edge and that of the latter is referred to as the bottom edge (See Figure 2). The radii investigated range from 0-15 μm, where this length denotes the radius of a cylinder tangent to both channel surfaces.

Finally, the channel depth and width were investigated. The channel depth is defined as the length from the plateau region to the bottom of the channel and the channel width is defined as the length of the channel bottom. Depths explored vary from 12-52 μm, and widths range from 22-62 μm. In each simulation performed, regardless of the parameter under scrutiny, the velocity field and shear stress were computationally elucidated as discussed earlier. This computational approach allows for rapid optimization of the geometric parameters described previously, resulting in the elucidation of microchannel models that experience wall shear stresses in the range of those found in native vessels.

Results

Channel models were created with the specified range of wall angles. For steady, laminar, low velocity over the models investigated, Comsol Multiphysics was used to define a mesh for the 3-D model. In order to create a computationally efficient model, the mesh was scaled so that the element size was at its smallest near the channel surface and the top edge and bottom edge of the channel. Upon solving the Navier-Stokes equation, the velocity profile for each model in question was generated when a velocity of 0.7 m/s in the x-direction is prescribed to the top of the 3-D model.

Effect of channel wall angle on wall shear stress

The channel wall angle was varied from 25º to 125.3º in order to determine the relationship between this geometric parameter and the wall shear stress in the channel. Figure 4 shows a representative velocity field for a V-shaped model with a wall angle of

45º (Panel A) and an inverted V-shaped model with a wall angle of 125.3º (Panel B). These velocity profiles are representative of those found for models of varying wall angle investigated in this study.

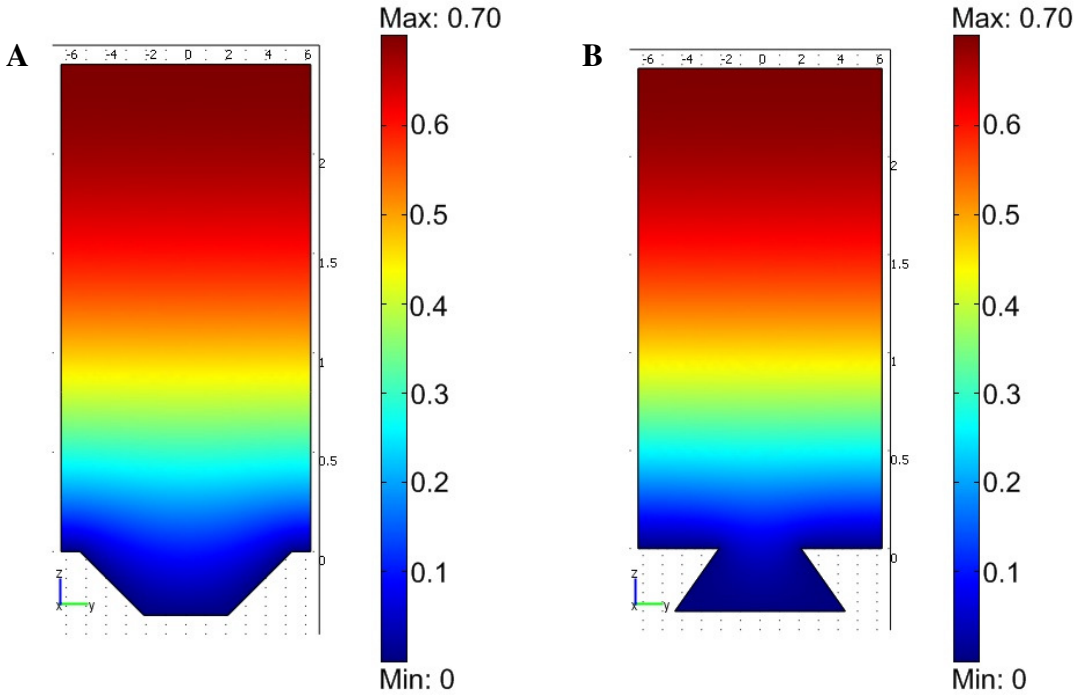

Figure 4. Representative velocity profiles for channel models with varying wall angle. Panel A shows a channel with a wall angle of 45º, depth of 32 µm, and width of 42 µm; while panel B shows a channel with a wall angle of 125.3º, depth of 32 µm, and width of 87.3 µm.

The velocity field in the channel itself is more easily observed when the velocity profile closer to the channel surfaces is examined by changing the range of velocity values shown on the model from 0-0.7 m/s to 0-0.015 m/s (Figure 5, A and B). Upon application of equation (8), the solutions for flow through the various channel models investigated were converted to wall shear stress in dyn/cm^2. Resulting wall shear stress values for the representative models shown in Figures 4 and 5 are as follows. The V-

shaped channel model with a wall angle of 45º had a maximum wall shear stress of 158 dyn/cm^2 at the top edges of the channel and an average wall shear stress on the channel bottom of 24 dyn/cm^2. A change in wall angle from this channel model to create an

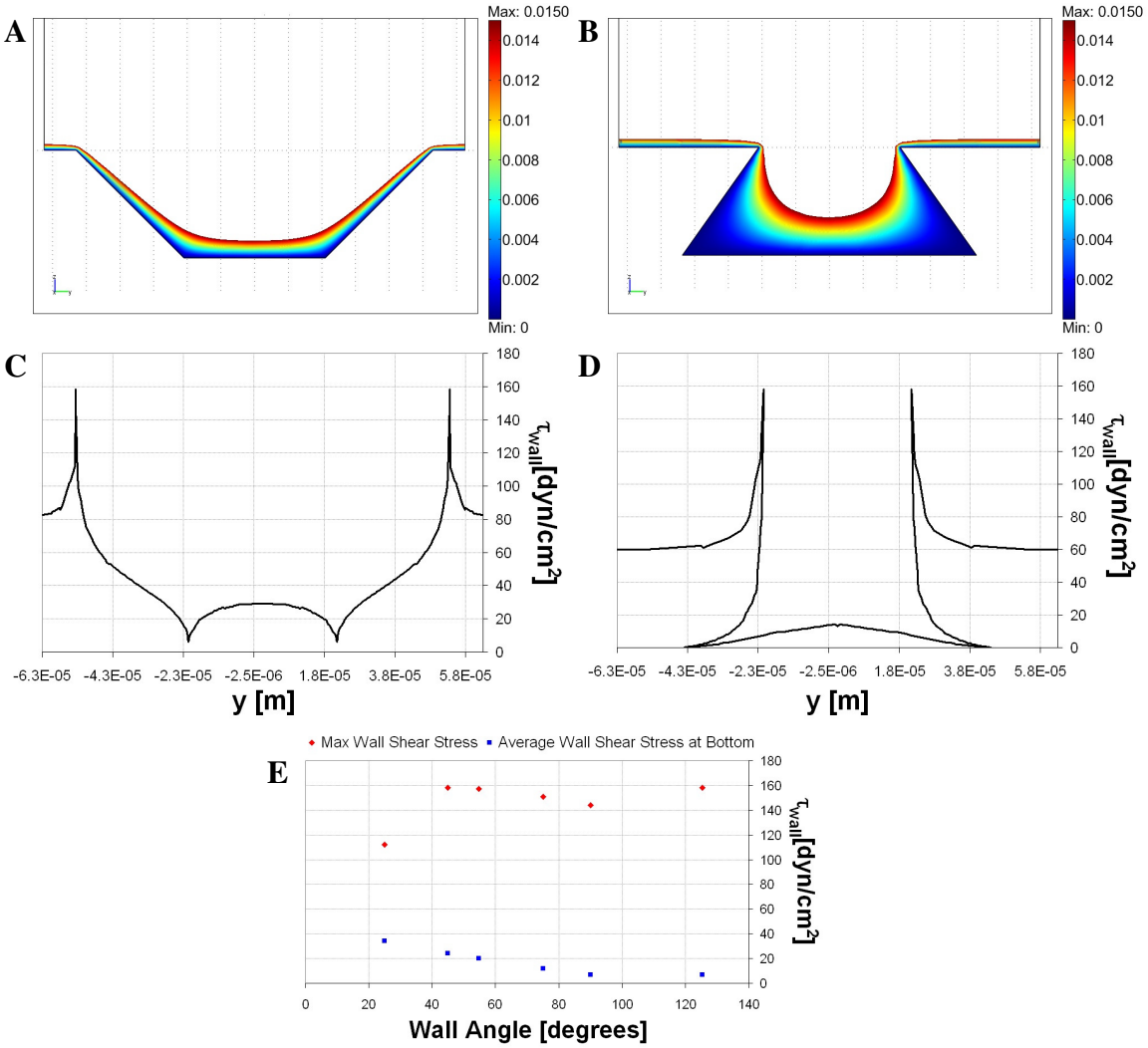

Figure 5. Effects of wall angle on wall shear stress. Panels A and B show a view of the velocity profile closer to the surface for wall angles of 45º and 125.3º, respectively. Panels C and D show the wall shear stress as a function of the horizontal position with these same two representative wall angles. Panel E shows the combined results for maximum wall shear stress and average wall shear stress on the channel bottom produced in microchannels with wall angles varying from 25º to 125.3º under steady, laminar flow. Maximum wall shear stress increases with increasing wall angle (red diamonds), however the average wall shear stress on the bottom decreases with this condition (blue squares).

inverted V-shaped channel with a wall angle of 125.3º, results in a maximum wall shear stress of 158 dyn/cm^2 and an average wall shear stress on the channel bottom of 7 dyn/cm^2. A plot of wall shear stress along the plateau, side wall and bottom for the 45º and 125.3º wall angles are as shown in panels C and D of Figure 5, in that order. For all models the location of maximum wall shear stress was at the transition between the plateau and the channel side wall (top edge). Figure 5, panel E shows a summary of the changes in maximum wall shear stresses, along with the average wall shear stress on the channel bottom, as the wall angle is increased from 25º to 125.3º. Maximum wall shear stress is shown to increase with increasing wall angle to an angle of about 45º, decrease slightly until a wall angle of 90º is reached, and then rise again as the wall angle continues to increase. The average wall shear stress on the channel bottom decreases and wall angle is increased. The inverted V-shaped channel models produce larger regions of low velocity flow, as observed in Figure 5B, when compared with the V-shaped channel models. These results indicate that a smaller channel wall angle is advantageous in producing physiological ranges of wall shear stress.

Effect of radius of curvature on wall shear stress

Investigation into the effects on shear stress when applying a smooth transition from the plateau region to the channel wall (top edge in Figure 2) and from the channel side wall to the channel bottom (bottom edge in Figure 2) was performed in the V-shaped channel model with a wall angle of 54.7º, a depth of 32 μm, and a width of 42 μm. Figure 6 shows representative near-surface velocity profiles for a channel model with a radius of curvature of 5 μm (panel A) and a channel model with a radius of curvature of 15 μm

(panel B). The wall shear stress plotted as a function of position in the channel is also shown for these two models (panels C and D). The maximum wall shear stress for a channel model with a radius of curvature of 5 μm is 121 dyn/cm^2, and the average wall

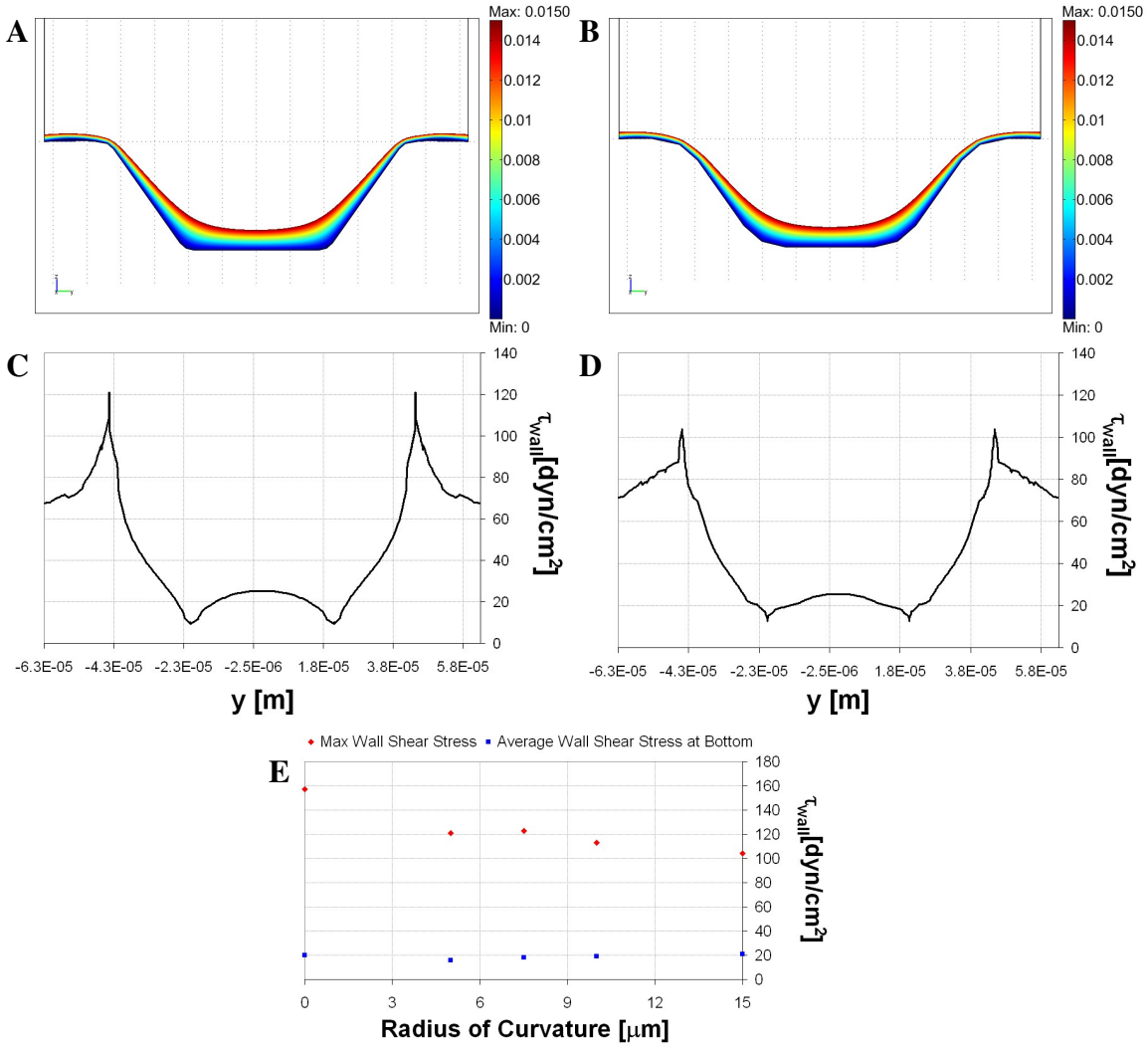

Figure 6. Effects of radius of curvature on wall shear stress. Panels A and B show a view of the velocity profile closer to the surface for both a radius of curvature of 5 μm and 15 μm, respectively. Panels C and D show the wall shear stress as a function of the horizontal position for each curvature. Variations in wall shear stress in a V-shaped microchannel model with a wall angle of 54.7º as a result of edge curvature are shown in panel E. The maximum wall shear stress (red diamonds) is shown to decrease with increasing radius of curvature. The average wall shear stress on the channel bottom (blue squares) was found to change minimally as the radius of curvature increases.

shear stress along the bottom is 16 dyn/cm^2. For a channel model with a radius of curvature of 15 μm, the maximum wall shear stress is 104 dyn/cm^2, and the average wall shear stress along the bottom is 21 dyn/cm^2. As the radius of curvature was increased at the top and bottom edges, a general decline in maximum wall shear stress resulted (see Figure 6E). The change in average wall shear stress at the channel bottom was relatively minor. These results indicate that introducing curvature at the top and bottom edges allows for a decrease in the peak wall shear stress at the top edge.

Effect of channel depth on wall shear stress

Another design parameter considered was the depth of the channel. The depth was varied from 12 to 52 μm in V-shaped channel models with a wall angle of 54.7º and a width of 42 μm. Examples of the near-surface velocity profiles are shown in Figure 7A and B corresponding to depths of 12 μm and 52 μm, respectively. The wall shear stress along the channel surface for each of these two channel models is shown in Figures 7C and D for the 12-μm and 52-μm deep channels, in that order. The maximum wall shear stress for a 12-μm deep channel was found to be 129 dyn/cm^2, and the average wall shear stress along the bottom of this channel is 32 dyn/cm^2. For a 52-μm deep channel, these values were found to be 173 dyn/cm^2 and 15 dyn/cm^2, respectively. Alterations in channel depth affect wall shear stress as shown in panel E of Figure 7. An increase in maximum wall shear stress is observed with increasing channel depth and a decrease in average wall shear stress on the channel bottom is seen as well.

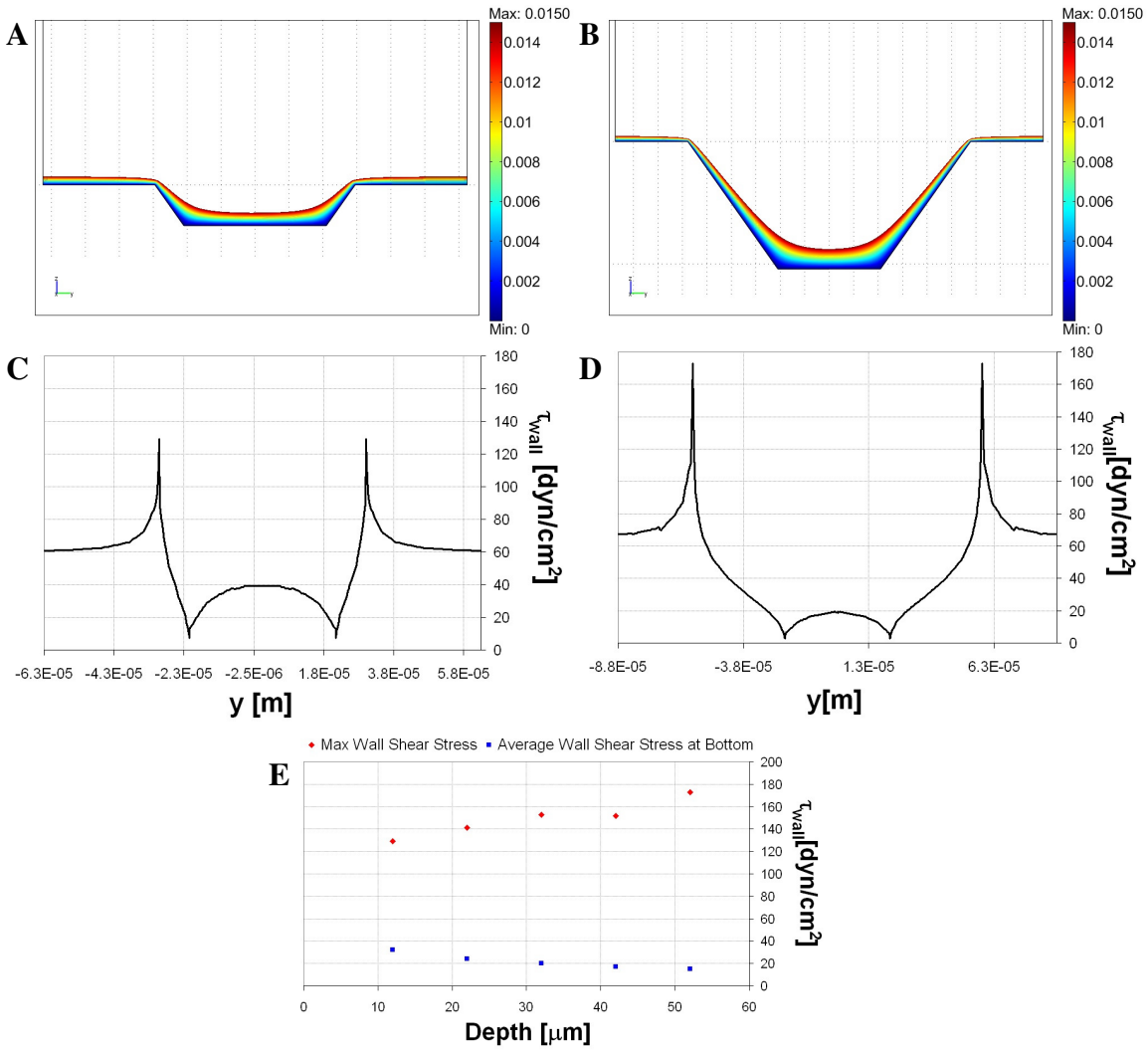

Figure 7. Channel depth effects on wall shear stress in V-Shaped microchannel with a wall angle of 54.7º and a width of 42 μm. Panels A and B show representative velocity profiles near the channel surface for models with depths of 12 μm and 52 μm, in that order. Panels C and D show the wall shear stress plotted against position in the channel for each of these two models. Panel E shows the resulting maximum shear stress and average wall shear stress along the bottom for all models investigated. As the channel depth increases, the maximum wall shear stress (red diamonds) rises, while the average wall shear stress at the bottom of the channel (blue squares) decreases.

Effect of channel width on wall shear stress

The next channel model design parameter examined was the width of the channel bottom. The width of a V-shaped channel model, with a wall angle of 54.7º and a depth

of 32 μm, was varied from 22 μm to 62 μm. Representative near-surface velocity profiles are shown in panels A and B of Figure 8 for the maximum and minimum widths in this range. The resulting maximum wall shear stress for each of these models was found to be

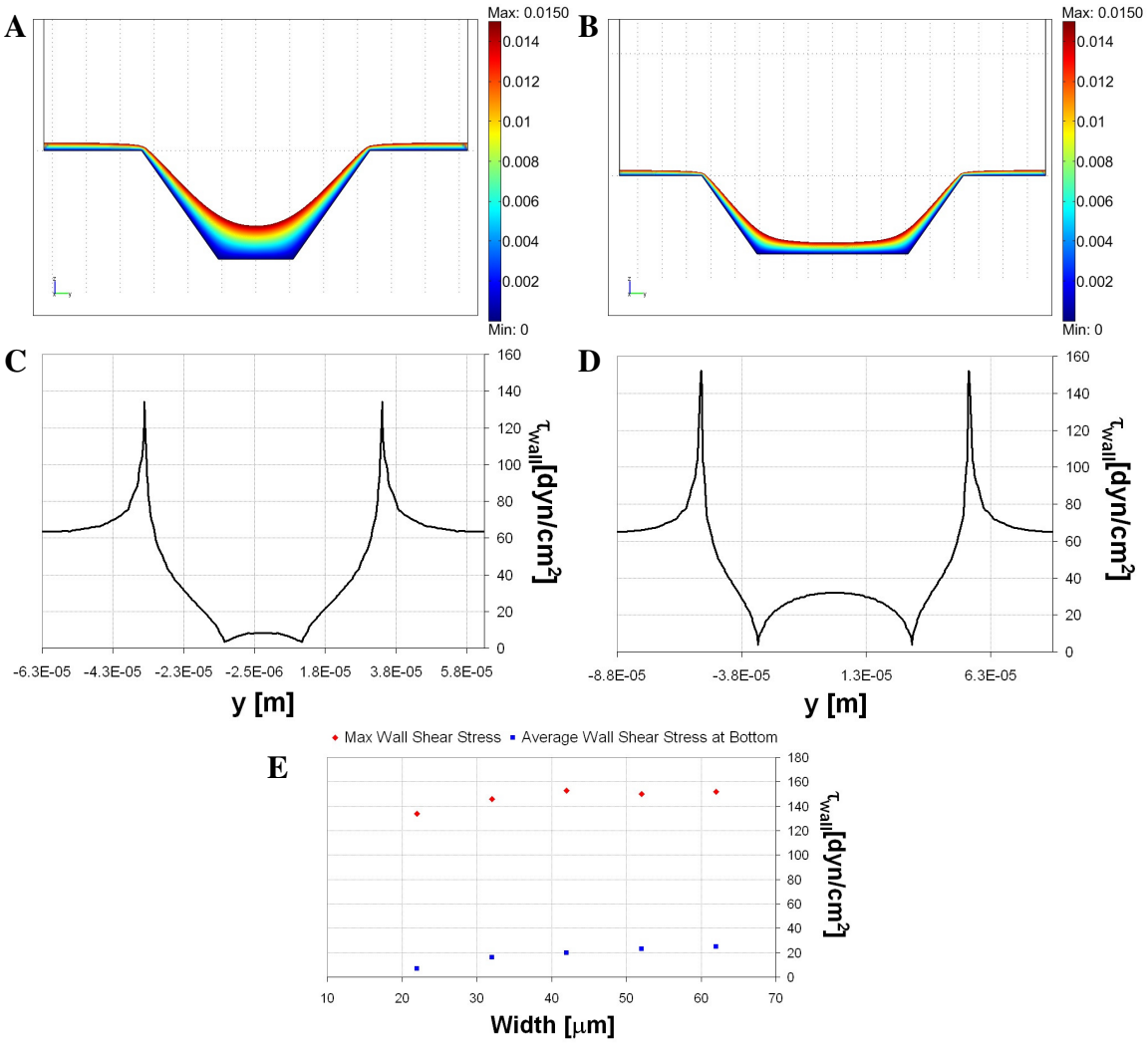

Figure 8. The effects of channel width on wall shear stress in V-Shaped microchannel with a wall angle of 54.7° and a depth of 32 μm. The velocity profile close to the channel surface is examined in panels A and B for models with widths of 22 μm and 62 μm, in that order. The wall shear stress in the two example channels is shown as a function of the position in the channel (panels C and D). Panel E shows the changes in wall shear stress for all widths explored. Increasing channel width is shown to result in an elevation in maximum wall shear stress (red diamonds), as well as a rise in the average wall shear stress at the channel bottom (blue squares)

134 dyn/cm^2 for a 22-μm wide channel and 152 dyn/cm^2 for a 62-μm wide channel. The average wall shear stress at the bottom for each is 7 dyn/cm^2 and 26 dyn/cm^2, respectively. Figure 8C and D show the changes in wall shear stress with position along the channel surfaces for each of these two representative models. When the width of channel bottom was increased, an increase in the maximum wall shear stress was seen. The average wall shear stress at the channel bottom also rose with increasing channel width (Figure 8E). A smaller channel bottom thus results in lower wall shear stress at both the top edge and along the channel bottom.

Optimal geometry

Since the goal of this work is to optimize the geometry of the microchannel, the effects of each parameter discussed above individually were combined to produce one of many possible models with wall shear stresses in the physiological range of 10-70 dyn/cm^2. The results above point to this optimized geometry consisting of a channel with a wall angle less than 45º and a radius of curvature of both the top and bottom edges of about 10 μm. Additionally, a shallow channel that is smaller in width is desirable. One possible optimal geometry was created to have a wall angle of 30º, radius of curvature at the top edge of 20 μm, radius of curvature at the bottom edge of 10 μm, depth of 5 μm, and width of 5 μm. The velocity profile (Figure 9) and wall shear stress were computationally elucidated as in all other models. Figure 9B shows the near-surface velocity profile for this model. The resulting maximum wall shear stress was found to be 68 dyn/cm^2 and the average wall shear stress at the channel bottom was 26 dyn/cm^2. Figure 9C shows the plot of wall shear stress along the channel walls. One can see with

comparison of this plot to the other walls shear stress plots shown earlier that there is a diminished peak in shear stress at the top edge of the channel and the absence of a minimum wall shear stress at the bottom edge. The new location of the minimum wall shear stress is at the center of the channel bottom, leading to an elevation in the average wall shear stress on the bottom of the channel. Although many 3-D models could be created that, when exposed to the same flow, would experience wall shear stress values in the physiological range, this model serves as an example of a geometry that has been optimized according to the defined set of parameters.

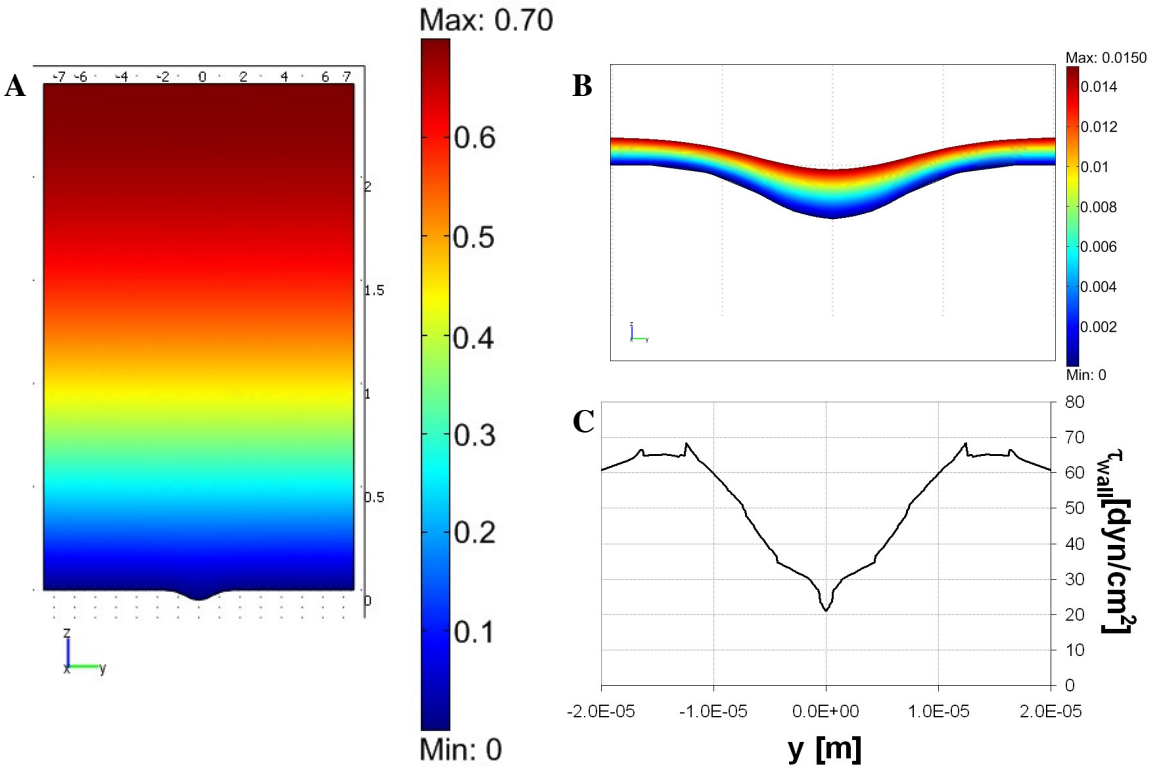

Figure 9. Optimal microchannel geometry. This channel is described by a wall angle of 30º, radius of curvature at the top edge of 20 µm, radius of curvature at the bottom edge of 10 µm, depth of 5 µm, and width of 5 µm. Panel A depicts the velocity field when a velocity of 1.5 m/s in the x-direction is located at the top of the channel geometry. Panel B gives a magnified view of this same velocity profile closer to the channel surface by adjusting the velocity range to 0-0.015 m/s. The plot of wall shear stress (Panel C) shows the maximum wall shear stress to be 146 dyn/cm^2 and the average wall shear stress at the channel bottom to be 56 dyn/cm^2.

Discussion

As discussed previously, physical surface modification of the synthetic vascular graft substrate is a potential method to achieve retention of endothelial cells when exposed to flow. Previous work has set the foundation for the use of computational fluid dynamics to assess microchannel geometry [56]. While capable of achieving significant retention, the microchannel geometry studied also exposed endothelial cells to low shear stresses, which are characteristic in regions prone to atherosclerosis. In attempt to simulate the physiological shear stress to which an endothelial cell is exposed *in vivo*, the channel geometry was optimized according to the criteria of reducing high wall shear stress regions at edges, while still maintaining substantial wall shear stress in the channel bottom to promote NO production. Factors that were investigated in order to meet these criteria include channel wall angle, radius of curvature of channel edges, channel depth, and channel width.

The wall angle was varied from 25º to 125.3º in a V-shaped channel with a depth of 32 μm and a width of 42 μm. As the wall angle is increased, a rise in the maximum wall shear stress is observed. At a wall angle of 25º the maximum wall shear stress is at the lowest point seen in the range of angles considered. The average wall shear stress along the channel bottom, however, decreases with increasing wall angle. A smaller wall angle, less than 65º, could potentially provide wall shear stresses closer to the physiological range. It is important to note that initially, and in the previous study [56], the wall angle of 54.7º was studied due to the ease in creating physical channels of this geometry by using typical anisotropic wet etching microfabrication techniques on a wafer

of (100) silicon. In order to produce channels with different wall angles, an alternate fabrication technique must be used, such as micromolding.

The study of the effect of curvature on wall shear stress was performed in the V-shaped channel model with a wall angle of 54.7º. In general, the greater the radius of curvature between the plateau and channel side wall and the channel side wall and channel bottom, the lower the maximum wall shear stress. A radius of curvature around 10 μm at both the top and bottom edges of the channel provides the lowest maximum wall shear stress seen for those radii considered and is thus considered optimal.

Increasing channel depth for the V-shaped model with a wall angle of 54.7º results in the increase of maximum wall shear stress while the average wall shear stress on the channel bottom decreases. Similarly, increasing the channel width also causes an increase in maximum wall shear stress, however an increase in average wall shear stress at the channel bottom is also observed. As the channel width is decreased, it is possible for the maximum wall shear stress to approach values typically found in a healthy vessel.

Shallow channels with small openings, gently rising walls, and rounded transitions between the plateaus, side walls, and bottoms give rise to a more physiological range of shear stresses. The optimal geometry modeled resulted in a range of wall shear stresses from 28-70 dyn/cm^2. This range only slightly deviates from the range of 10-70 dyn/cm^2 as reported by [58]. Because endothelial cells require shear stress for normal function, those channels revealing areas of low wall shear stresses (<10dyn/cm^2) are not optimal for cell seeding. Conversely, high wall shear stress may result in either the shearing of endothelial cells from the surface or shear induced platelet adhesion, both leading to thrombus formation and graft failure. Endothelial cell sensitivity to shear stress

requires that graft surfaces be designed in such a way as to expose the cell to a range of stresses that will support its adhesion and normal function.

CHAPTER III

DISCUSSION

Summary

The current work has successfully identified elements of surface topography of a vascular graft lumen that may promote endothelial cell survival and retention under flow conditions. By creating a pattern of channels on the surface of a substrate for seeding endothelial cells, it is possible to create regions of diminished shear stress, thus allowing for the reduction of delamination [56]. One flaw of the channel design of the previous work was the presence of elevated wall shear stress localized along the channel edges (where the valleys meet the plateaus). Another issue in the previous design was the presence of regions of stagnant flow in the channel bottoms. In order to address both of these concerns, the channel model geometry was altered in such a way as to select for a range of wall shear stress. It should be noted that flow rates, and subsequent wall shear stress values, vary throughout the arterial circulation based on such parameters as vessel diameter, vessel curvature, and presence of bifurcations, which cause flow separation. Importantly, the technique used in the current work can be readily adapted to account for local flow conditions at the site of grafting through the use of computational fluid dynamics simulations. The range of shear stresses for a normal artery, as reported by Malek *et al.*, is 10-70 dyn/cm^2 [58]. The production of NO has also been shown to increase over a range of shear stress between 1 and 10 dyn/cm^2 [70], indicating that a sufficient level of shear stress must be present for NO synthesis to occur. Altering the

depth, width, wall angle, and curvature at edges resulted in changes in the flow field. Consequently, differing wall shear stress values were calculated for each unique channel model that was tested. With all models investigated, the location of peak wall shear stress was at the top edges of the channel and the location of minimum shear stress was at the channel bottoms. The channel model, among those explored, that best fit the range of desired wall shear stress was the geometry shown in Figure 9 with both a depth and width of 5 μm, a wall angle of 30º, a top edge radius of curvature of 20 μm, and a bottom edge radius of curvature of 10 μm.

In the work of Uttayarat *et al.* [51] in which vertically walled channels of varying depths were compared, it was suggested that endothelial cells sense topographic features as small as 200 nm and appear to alter their morphology to follow the surface topography. They found that cell alignment in a 1-μm deep channel was superior both to shallower channels and to deeper channels. However, the width of the channel was not held constant, and thus, they speculate this may have altered the experimental trends. This work provides experimental evidence of enhanced endothelial cell alignment and enhanced focal adhesion attachment in channels of similar sizes to those studied in the current work. It is likely that endothelial cells seeded on substrates patterned with the optimal channel geometry developed in this work will adhere and align in a similar manner.

Although there is little work done in the area of endothelial cell retention on patterned surfaces when exposed to arterial flow rates, the previous work done in our lab has shown significantly improved retention of cells seeded on a micropatterned surface when exposed to flow conditions [56]. It is based on this work that one would expect

similar, if not increased retention of endothelial cells when seeded on substrates patterned with the optimal geometry found in the current work. In order to create an environment within the range of physiological stresses, optimization of the specific geometry of the luminal surface was performed leading to the reduction of peak wall shear stresses and to the increase in the average wall shear stress on the channel bottom from the previous work in our laboratory to the current work. It is expected that these modifications will promote normal endothelial cell function and improved retention.

Future Work

The next phase of this study will involve the creation of the optimal geometry by micromolding techniques in which a stamp is used to pattern a substrate. One specific aim will consist of comparing platelet adhesion to unseeded, optimally patterned substrates with the extent of platelet adhesion to an unpatterned surface. This will be done with the use of a parallel plate flow chamber perfused with whole blood or platelet-rich plasma. In the next specific aim endothelial cells will be seeded on the surface of the patterned substrate and parallel plate flow studies will be again be performed in order to determine if the geometry is capable of enhancing retention as compared with a non-patterned surface. During this span of experimentation, it will be possible to also determine the effect of a fibronectin coating or a covalently bound RGD peptide on the adhesion of endothelial cells. Additionally, the role of endothelial cell culture time on the attachment of cells may be assessed in terms of F-actin and focal adhesions as done by Uttayarat *et al.* [51]. The effect of preconditioning on endothelial cell retention to micropatterned surfaces may be assessed *in vitro* and *in vivo*. A potential animal model

for the implantation of these unique surfaces as the sub-endothelium of a vascular graft would be the New Zealand white rabbit. In order to test the patency of these grafts, a short-term trial, with a time period of weeks to a couple months, could be conducted initially, followed by a long-term trial lasting for over a year. Upon removal of the implanted graft, the endothelial cell coverage, thrombosis, and intimal thickness will be assessed. Of course it is desired that grafts employing a micropatterned surface for enhanced retention of endothelial cells will prove to show long-term patency, however until the reminder of the experiments in this plan come to fruition, the search for a clinically useful small-diameter vascular graft continues.

REFERENCES

1. Anderson, R.N. and B.L. Smith, *Deaths: leading causes for 2002.* Natl Vital Stat Rep, 2005. **53**(17): p. 1-89.

2. Lefkowitz, R.J. and J.T. Willerson, *Prospects for cardiovascular research.* Jama, 2001. **285**(5): p. 581-7.

3. Furberg, C.D., *Natural statins and stroke risk.* Circulation, 1999. **99**(2): p. 185-8.

4. Brener, S.J., et al., *Propensity analysis of long-term survival after surgical or percutaneous revascularization in patients with multivessel coronary artery disease and high-risk features.* Circulation, 2004. **109**(19): p. 2290-5.

5. Blumenthal, R.S., G. Cohn, and S.P. Schulman, *Medical therapy versus coronary angioplasty in stable coronary artery disease: a critical review of the literature.* J Am Coll Cardiol, 2000. **36**(3): p. 668-73.

6. Baim, D.S., *Percutaneous treatment of saphenous vein graft disease: the ongoing challenge.* J Am Coll Cardiol, 2003. **42**(8): p. 1370-2.

7. de Feyter, P.J., J. Vos, and B.J. Rensing, *Anti-restenosis Trials.* Curr Interv Cardiol Rep, 2000. **2**(4): p. 326-331.

8. Sherwood, L., *Human physiology: from cells to systems*. 4th ed. 2001, Pacific Grove, Calif.: Brooks/Cole. xx, 766 p.

9. Wu, K.K., *Platelet activation mechanisms and markers in arterial thrombosis.* J Intern Med, 1996. **239**(1): p. 17-34.

10. Conte, M.S., *The ideal small arterial substitute: a search for the Holy Grail?* Faseb J, 1998. **12**(1): p. 43-5.

11. Eagle, K.A., et al., *ACC/AHA 2004 guideline update for coronary artery bypass graft surgery: summary article. A report of the American College of Cardiology/American Heart Association Task Force on Practice Guidelines (Committee to Update the 1999 Guidelines for Coronary Artery Bypass Graft Surgery).* J Am Coll Cardiol, 2004. **44**(5): p. e213-310.

12. Isenberg, B.C., C. Williams, and R.T. Tranquillo, *Small-diameter artificial arteries engineered in vitro.* Circ Res, 2006. **98**(1): p. 25-35.

13. Nerem, R.M. and D. Seliktar, *Vascular tissue engineering.* Annu Rev Biomed Eng, 2001. **3**: p. 225-43.

14. Seifalian, A.M., et al., *Improving the clinical patency of prosthetic vascular and coronary bypass grafts: the role of seeding and tissue engineering.* Artif Organs, 2002. **26**(4): p. 307-20.

15. Rashid, S.T., et al., *Engineering of bypass conduits to improve patency.* Cell Prolif, 2004. **37**(5): p. 351-66.

16. Baguneid, M.S., et al., *Tissue engineering of blood vessels.* Br J Surg, 2006. **93**(3): p. 282-90.

17. Kannan, R.Y., et al., *Current status of prosthetic bypass grafts: a review.* J Biomed Mater Res B Appl Biomater, 2005. **74**(1): p. 570-81.

18. Kaushal, S., et al., *Functional small-diameter neovessels created using endothelial progenitor cells expanded ex vivo.* Nat Med, 2001. **7**(9): p. 1035-40.

19. Teebken, O.E., A.M. Pichlmaier, and A. Haverich, *Cell seeded decellularised allogeneic matrix grafts and biodegradable polydioxanone-prostheses compared with arterial autografts in a porcine model.* Eur J Vasc Endovasc Surg, 2001. **22**(2): p. 139-45.

20. Hoenig, M.R., et al., *Tissue-engineered blood vessels: alternative to autologous grafts?* Arterioscler Thromb Vasc Biol, 2005. **25**(6): p. 1128-34.

21. Teebken, O.E. and A. Haverich, *Tissue engineering of small diameter vascular grafts.* Eur J Vasc Endovasc Surg, 2002. **23**(6): p. 475-85.

22. Shum-Tim, D., et al., *Tissue engineering of autologous aorta using a new biodegradable polymer.* Ann Thorac Surg, 1999. **68**(6): p. 2298-304; discussion 2305.

23. Niklason, L.E., et al., *Functional arteries grown in vitro.* Science, 1999. **284**(5413): p. 489-93.

24. Matsumura, G., et al., *Successful application of tissue engineered vascular autografts: clinical experience.* Biomaterials, 2003. **24**(13): p. 2303-8.

25. Watanabe, M., et al., *Tissue-engineered vascular autograft: inferior vena cava replacement in a dog model.* Tissue Eng, 2001. **7**(4): p. 429-39.

26. Weinberg, C.B. and E. Bell, *A blood vessel model constructed from collagen and cultured vascular cells.* Science, 1986. **231**(4736): p. 397-400.

27. Seifalian, A.M., et al., *In vivo biostability of a poly(carbonate-urea)urethane graft.* Biomaterials, 2003. **24**(14): p. 2549-57.

28. L'Heureux, N., et al., *A completely biological tissue-engineered human blood vessel.* Faseb J, 1998. **12**(1): p. 47-56.

29. Kidane, A.G., et al., *Anticoagulant and antiplatelet agents: their clinical and device application(s) together with usages to engineer surfaces.* Biomacromolecules, 2004. **5**(3): p. 798-813.

30. Keuren, J.F., et al., *Covalently-bound heparin makes collagen thromboresistant.* Arterioscler Thromb Vasc Biol, 2004. **24**(3): p. 613-7.

31. Aldenhoff, Y.B. and L.H. Koole, *Platelet adhesion studies on dipyridamole coated polyurethane surfaces.* Eur Cell Mater, 2003. **5**: p. 61-7; discussion 67.

32. Yoneyama, T., et al., *Small diameter vascular prosthesis with a nonthrombogenic phospholipid polymer surface: preliminary study of a new concept for functioning in the absence of pseudo- or neointima formation.* Artif Organs, 2000. **24**(1): p. 23-8.

33. Herring, M., A. Gardner, and J. Glover, *A single-staged technique for seeding vascular grafts with autogenous endothelium.* Surgery, 1978. **84**(4): p. 498-504.

34. Bos, G.W., et al., *Small-diameter vascular graft prostheses: current status.* Arch Physiol Biochem, 1998. **106**(2): p. 100-15.

35. Pawlowski, K.J., et al., *Endothelial cell seeding of polymeric vascular grafts.* Front Biosci, 2004. **9**: p. 1412-21.

36. Salacinski, H.J., et al., *Cellular engineering of vascular bypass grafts: role of chemical coatings for enhancing endothelial cell attachment.* Med Biol Eng Comput, 2001. **39**(6): p. 609-18.

37. Deutsch, M., et al., *Clinical autologous in vitro endothelialization of infrainguinal ePTFE grafts in 100 patients: a 9-year experience.* Surgery, 1999. **126**(5): p. 847-55.

38. Bhat, V.D., G.A. Truskey, and W.M. Reichert, *Fibronectin and avidin-biotin as a heterogeneous ligand system for enhanced endothelial cell adhesion.* J Biomed Mater Res, 1998. **41**(3): p. 377-85.

39. Cook, A.D., et al., *Characterization and development of RGD-peptide-modified poly(lactic acid-co-lysine) as an interactive, resorbable biomaterial.* J Biomed Mater Res, 1997. **35**(4): p. 513-23.

40. Massia, S.P. and J.A. Hubbell, *Human endothelial cell interactions with surface-coupled adhesion peptides on a nonadhesive glass substrate and two polymeric biomaterials.* J Biomed Mater Res, 1991. **25**(2): p. 223-42.

41. Lin, H.B., et al., *Endothelial cell adhesion on polyurethanes containing covalently attached RGD-peptides.* Biomaterials, 1992. **13**(13): p. 905-14.

42. Lin, H.B., et al., *Synthesis, surface, and cell-adhesion properties of polyurethanes containing covalently grafted RGD-peptides.* J Biomed Mater Res, 1994. **28**(3): p. 329-42.

43. Massia, S.P. and J. Stark, *Immobilized RGD peptides on surface-grafted dextran promote biospecific cell attachment.* J Biomed Mater Res, 2001. **56**(3): p. 390-9.

44. Hubbell, J.A., et al., *Endothelial cell-selective materials for tissue engineering in the vascular graft via a new receptor.* Biotechnology (N Y), 1991. **9**(6): p. 568-72.

45. Jun, H.W. and J.L. West, *Modification of polyurethaneurea with PEG and YIGSR peptide to enhance endothelialization without platelet adhesion.* J Biomed Mater Res B Appl Biomater, 2005. **72**(1): p. 131-9.

46. Ott, M.J. and B.J. Ballermann, *Shear stress-conditioned, endothelial cell-seeded vascular grafts: improved cell adherence in response to in vitro shear stress.* Surgery, 1995. **117**(3): p. 334-9.

47. Isenberg, B.C., C. Williams, and R.T. Tranquillo, *Endothelialization and flow conditioning of fibrin-based media-equivalents.* Ann Biomed Eng, 2006. **34**(6): p. 971-85.

48. Dardik, A., A. Liu, and B.J. Ballermann, *Chronic in vitro shear stress stimulates endothelial cell retention on prosthetic vascular grafts and reduces subsequent in vivo neointimal thickness.* J Vasc Surg, 1999. **29**(1): p. 157-67.

49. Baguneid, M., et al., *Shear-stress preconditioning and tissue-engineering-based paradigms for generating arterial substitutes.* Biotechnol Appl Biochem, 2004. **39**(Pt 2): p. 151-7.

50. Riha, G.M., et al., *Roles of hemodynamic forces in vascular cell differentiation.* Ann Biomed Eng, 2005. **33**(6): p. 772-9.

51. Uttayarat, P., et al., *Topographic guidance of endothelial cells on silicone surfaces with micro- to nanogrooves: orientation of actin filaments and focal adhesions.* J Biomed Mater Res A, 2005. **75**(3): p. 668-80.

52. Gray, D.S., J. Tien, and C.S. Chen, *Repositioning of cells by mechanotaxis on surfaces with micropatterned Young's modulus.* J Biomed Mater Res A, 2003. **66**(3): p. 605-14.

53. Goodman, S.L., P.A. Sims, and R.M. Albrecht, *Three-dimensional extracellular matrix textured biomaterials.* Biomaterials, 1996. **17**(21): p. 2087-95.

54. Fujisawa, N., et al., *A novel textured surface for blood-contact.* Biomaterials, 1999. **20**(10): p. 955-62.

55. Bettinger, C.J., et al., *Microfabrication of poly (glycerol-sebacate) for contact guidance applications.* Biomaterials, 2006. **27**(12): p. 2558-65.

56. Daxini, S.C., et al., *Micropatterned polymer surfaces improve retention of endothelial cells exposed to flow-induced shear stress.* Biorheology, 2006. **43**(1): p. 45-55.

57. Dewey, C.F., Jr., et al., *The dynamic response of vascular endothelial cells to fluid shear stress.* J Biomech Eng, 1981. **103**(3): p. 177-85.

58. Malek, A.M., S.L. Alper, and S. Izumo, *Hemodynamic shear stress and its role in atherosclerosis.* Jama, 1999. **282**(21): p. 2035-42.

59. Traub, O. and B.C. Berk, *Laminar shear stress: mechanisms by which endothelial cells transduce an atheroprotective force.* Arterioscler Thromb Vasc Biol, 1998. **18**(5): p. 677-85.

60. Wootton, D.M. and D.N. Ku, *Fluid mechanics of vascular systems, diseases, and thrombosis.* Annu Rev Biomed Eng, 1999. **1**: p. 299-329.

61. Dimmeler, S., et al., *Activation of nitric oxide synthase in endothelial cells by Akt-dependent phosphorylation.* Nature, 1999. **399**(6736): p. 601-5.

62. Kaiser, D., M.A. Freyberg, and P. Friedl, *Lack of hemodynamic forces triggers apoptosis in vascular endothelial cells.* Biochem Biophys Res Commun, 1997. **231**(3): p. 586-90.

63. Dimmeler, S., et al., *Shear stress inhibits apoptosis of human endothelial cells.* FEBS Lett, 1996. **399**(1-2): p. 71-4.

64. Frangos, J., L. McIntire, and S. Eskin, *Shear Stress Induced Stimulation of Mammalian Cell Metabolism.* Biotechnology and Bioengineering, 1988. **32**(8): p. 1053-1060.

65. Levesque, M.J. and R.M. Nerem, *The elongation and orientation of cultured endothelial cells in response to shear stress.* J Biomech Eng, 1985. **107**(4): p. 341-7.

66. Chappell, D.C., et al., *Oscillatory shear stress stimulates adhesion molecule expression in cultured human endothelium.* Circ Res, 1998. **82**(5): p. 532-9.

67. Gaver, D.P., 3rd and S.M. Kute, *A theoretical model study of the influence of fluid stresses on a cell adhering to a microchannel wall.* Biophys J, 1998. **75**(2): p. 721-33.

68. Usha, R., S. Senthilkumar, and E.G. Tulapurkara, *Numerical study of particulate suspension flow through wavy-walled channels.* INTERNATIONAL JOURNAL FOR NUMERICAL METHODS IN FLUIDS, 2006. **51**: p. 235-259.

69. Tai, N.R., et al., *Compliance properties of conduits used in vascular reconstruction.* Br J Surg, 2000. **87**(11): p. 1516-24.

70. Nerem, R.M., et al., *The study of the influence of flow on vascular endothelial biology.* Am J Med Sci, 1998. **316**(3): p. 169-75.